

Determination of equivalent blasting load considering millisecond delay effect

Zhan-Ping Song^{1,2}, Shi-Hao Li¹, Jun-Bao Wang^{*1}, Zhi-Yuan Sun³, Jing Liu¹ and Yu-Zhen Chang¹

¹School of Civil Engineering, Xi'an University of Architecture and Technology, Xi'an, China

²Research Center of the Tunnel and Underground Structure Engineering, Xi'an University of Architecture and Technology, Xi'an, China

³Chinese Railway Bridge Engineering Bureau Group Co. Ltd., Tianjin, China

(Received August 7, 2017, Revised November 20, 2017, Accepted November 29, 2017)

Abstract. In the analysis of the effects of rock tunnel blasting vibration on adjacent existing buildings, the model of simplified equivalent load produces higher calculation result of vibration, due to the lack of consideration of the millisecond delay effect. This paper, based on the static force equivalence principle of blasting load, proposes a new determination method of equivalent load of blasting vibration. The proposed method, based on the elastic-static force equivalence principle of stress wave, equals the blasting loads of several single blastholes in the same section of millisecond blasting to the triangle blasting load curve of the exploded equivalent elastic boundary surface. According to the attenuation law of stress wave, the attenuated equivalent triangle blasting load curve of the equivalent elastic boundary is applied on the tunnel excavation contour surface, obtaining the final applied equivalent load. Taking the millisecond delay time of different sections into account, the time-history curve of equivalent load of the whole section applied on the tunnel excavation contour surface can be obtained. Based on Sailing Tunnel with small spacing on Sanmenxia-Xichuan Expressway, an analysis on the blasting vibration response of the later and early stages of the tunnel construction is carried out through numerical simulation using the proposed equivalent load model considering millisecond delay effect and the simplified equivalent triangle load curve model respectively. The analysis of the numerical results comparing with the field monitoring ones shows that the calculation results obtained from the proposed equivalent load model are closer to the measured ones and more feasible.

Keywords: tunnel; millisecond blasting; delay effect; equivalent load

1. Introduction

Drilling and Blasting has been widely applied into tunnel construction for its flexible construction method and high applicability and economical efficiency (Ak *et al.* 2009, Cardu and Seccatore 2016). However, its limitation lies in that it exerts a large influence on the surroundings, especially the vibration of adjacent existing buildings (Song *et al.* 2016). Thus, the accurate evaluation and prediction of the effects of blasting vibration on adjacent existing buildings have been a hot issues in tunnel engineering construction (Rodríguez *et al.* 2007, Ozer 2008, Nateghi *et al.* 2009, Ramulu *et al.* 2009, Kuzu and Guclu 2009, Jiang and Zhou 2012).

Numerical modeling, which is commonly used to analyze the effect of blasting vibration on adjacent existing buildings, can be realized in two approaches. The first approach is to simulate the detonation of explosive and the interaction between detonation products and rock through the equations of explosive property and state and thus analyze the vibration of surrounding media and the vibration propagation in rock during the blasting. For instance, in LS-DYNA, JWL (Jones-Wilkins-Lee) equation of state is used to simulate the explosion process (Saharan and Mitri 2008, Banadaki and Mohanty 2012, Sainoki and

Mitri 2014). The problem is that apart from the complicated explosion process of tunnel project and the variable surrounding rocks, the blasthole modeling needs a huge amount of model elements to simulate tunnel multi-blasthole explosion. Thus, it is extremely difficult to calculate dynamically through the first approach. The second approach believes that the effect of blasting vibration is actually the dynamic response of the tunnel surrounding rock to blasting dynamic load. Thus, based on the premise that the effect of blasting vibration is equivalent to a dynamic load applied on the tunnel excavation contour line, a dynamic time-history analysis is carried out in the second approach (Yang *et al.* 2013). Irrespective of the specific process of explosive blasting, this approach significantly reduces the calculation of multi-blasthole explosion in practical project. However, it needs to determine the time-history curve of equivalent blasting load. In terms of the simulation of tunnel blasting load, an equivalent load curve obtained by multiplying peak load by time-history function is widely used internationally (Ma and An 2008, Yilmaz and Unlu 2013). While in China, a semi-theoretical and semi-empirical triangle load curve is commonly used to simplify the applying process of blasting load (Li *et al.* 2010). The triangle load curve is widely applied in the response analysis of tunnel blasting vibration due to simple and convenient applying method of blasting vibration as well as clear physical process. However, the calculation results of blasting vibration are far larger than the measured ones as the triangle load curve fails to consider the applying process of dynamic load caused by

*Corresponding author, Associate Professor
E-mail: xajdwangjunbao@163.com

the initiation time intervals of different sections in the initiation process of millisecond blasting.

To accurately evaluate and predict the effects of blasting vibration on adjacent existing buildings, this paper, based on the equivalent elastic boundary put forward by Lu *et al.* (2011), considering the delay and vibration-isolating effects of millisecond blasting, proposes a time-history curve determination method of blasting load and verifies its rationality through the measured data of Sailing Tunnel on Sanmenxia-Xichuan Expressway.

2. Simulation computations and loading of blasting load

To analyze the effects of tunnel blasting vibration on adjacent existing buildings (constructions) through numerical simulation, the actual tunnel blasting should be simplified into a reasonable blasting load model in which the peak load, applying position, loading direction, occurrence time of peak load, and loading time should be determined. Apart from those, the attenuation function of blasting load should be determined as well (Lu *et al.* 2011, 2012).

2.1 Simplified model of tunnel blasting load

Currently, there are two simplified models of tunnel blasting load: the “single blasthole load model”, using a semi-theoretical and semi-experimental method, directly applies the time-history curve of pressure of single blasthole obtained through the explosive parameters during tunnel blasting on the blasthole wall; the “multi-blasthole load model”, based on the equivalent principle of force and considering the positions and amount of blastholes when the tunnel face explodes, applies the equivalently simplified blasting loads of several blastholes on the excavation boundary of tunnel. The pressure rising time, unloading time, and peak and attenuation function of blasting load need to be determined first in both methods.

(1) Peak load on the blasthole wall

Based on the condensed explosive detonation wave Chapman-Jouguet theory (Henrych 1979) the peak value of blasting load of single blasthole P_0 can be obtained from Eq. (1).

$$P_0 = \frac{\rho_e D^2}{2(\gamma + 1)} \quad (1)$$

where ρ_e and D respectively are the density and detonation velocity of explosive, and γ is entropic exponent which is related to charge density. When $\rho_e < 1.2 \text{g/cm}^3$, $\gamma = 2.1$; when $\rho_e \geq 1.2 \text{g/cm}^3$, $\gamma = 3$.

For change structure which decouples in radial and axial directions or has small decoupling coefficient, the peak load on the blasthole wall can be obtained from Eqs. (2) and (3).

$$P_0 = \frac{\rho_e D^2}{2(\gamma + 1)} (\zeta)^{2\gamma} \left(\frac{l_e}{l_b} \right)^\gamma n \quad (2)$$

$$\zeta = r_1 / r_0 \quad (3)$$

where ζ is the decoupling coefficient of charge ($\zeta = r_1 / r_0$), r_1

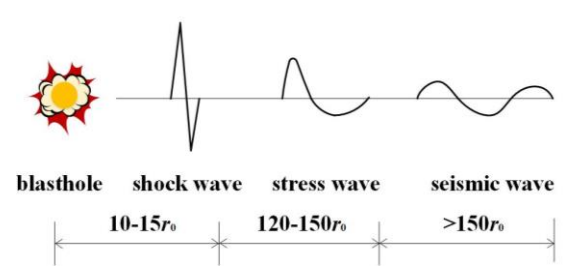


Fig. 1 The process of stress wave propagation

is the charge radius, r_0 is the radius of blasthole, l_e is the total length of grain, l_b is the depth of blasthole, and n is the enlargement factor of pressure when the detonation products crush against blasthole wall in high velocity. Generally, n ranges from 8 to 11.

If the decoupling coefficient is large, the gas expansion will go through two stages, namely, $P \geq P_c$ and $P < P_c$. P_c is the critical pressure of gas (Lu *et al.* 2012). γ is regarded as a piecewise constant in calculation. When $P \geq P_c$, $\gamma = 3.0$; when $P < P_c$, $\gamma = \nu = 4/3$. ν is the isentropic exponent of detonation gas (Ling and Li 2004). Then Eq. (2) can be developed into

$$P_0 = \left[\frac{\rho_0 D^2}{2(\gamma + 1)} \right]^{\nu/\gamma} P_c^{(\gamma - \nu)/\gamma} \left(\frac{r_1}{r_2} \right)^{2\nu} \quad (4)$$

(2) The pressure rising time and unloading time of blasting load

The pressure rising time and unloading time of blasting load are related to such factors as charge quantity, mechanical properties of rock, distance between explosive and blasthole wall and can respectively be worked out through the empirical formula (Wang 1984) below

$$t_r = \frac{12\sqrt{r^{2-\mu}} Q^{0.05}}{K} \quad (5)$$

$$t_s = \frac{84\sqrt{r^{2-\mu}} Q^{0.2}}{K} \quad (6)$$

where r is the ratio of distance from the blasthole center R to blasthole diameter r_0 ($r = R / r_0$), μ is the Poisson's ration of rock, K is the compression modulus of rock volume (kg/cm^2), and Q is the charge quantity of blasthole in one section.

The unloading time of blasting load can be obtained by subtracting Eq. (5) from Eq. (6).

(3) Attenuation function of blasting load

The detonation wave caused by explosive blast lashes violently against the blasthole wall, leading to the crush of surrounding rocks (the failure zone is 5 times the diameter of blasthole) and a shock wave in area near the explosion source (Li *et al.* 2016). The shock wave attenuates rapidly in rocks and gradually develops into compressive stress wave when it reaches $10-15r_0$ away from the explosion source. The compressive stress wave becomes less destructive, leading to the tensile-share failure of rock. As the compressive stress wave propagates, it will gradually attenuate and develop into seismic wave in rock. The

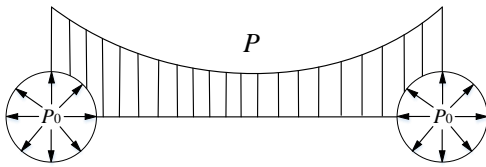


Fig. 2 Stress distribution of blastholes

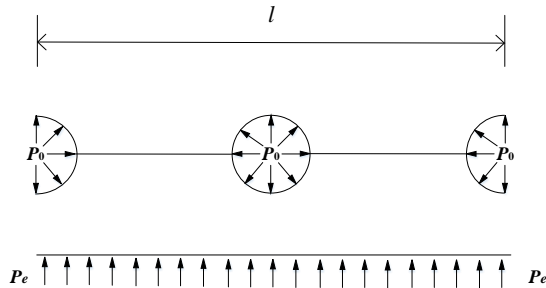


Fig. 3 Distribution of equivalent load

seismic wave is not so destructive and thus it only causes the shake of rock, which will pull the cracks in rock further apart (Sanchidrian *et al.* 2007, Resende *et al.* 2010, Resende *et al.* 2014). The propagation process of stress wave in rock is shown in Fig. 1.

The attenuation law (Henrych 1979) of blasting load in rock meets Eq. (7), namely

$$P_b = P \left(\frac{r_0}{R} \right)^\alpha \quad (7)$$

where P is the blasting load on blasthole wall, R is the distance from the blasthole center and α is the attenuation index of load propagation.

The empirical correlation between the stress attenuation index and Poisson's ratio of rock proposed by former Soviet Union scholars is expressed as

$$\alpha = 2 \pm \frac{\mu}{1 - \mu} \quad (8)$$

In the shock wave zone, $\alpha = 2 + \mu / (1 - \mu)$; in the stress wave zone, $\alpha = 2 - \mu / (1 - \mu)$.

(4) Description and simplification of multi-blasthole load model

Under violent explosion, the area near the exploded rocks undergoes extremely complicated stress-strain process, including detonation wave striking blasthole wall, blast wave crushing rock, and compressive stress wave pulling rocks apart (Wang 1984). According to the propagation process of stress wave in rocks caused by explosion, the complicated loads near the exploded area is regarded as a resultant force applied on the equivalent elastic boundary so as to simulate the situations of multi-blasthole detonation. As the detonation wave strikes blasthole wall, the rocks around the blasthole wall will crush, and the blast wave will attenuate and transform into stress wave which acts on crushing zone. The stress distribution between two adjacent blastholes is shown in Fig. 2. According to Saint-Venant's Principle, the stress

caused by the loads on a small part of elastomer is related to the resultant force of loads in regions away from the loads. Therefore, the load on the blasthole wall can be evenly distributed along the line between blastholes. The distribution of equivalent load is shown in Fig. 3. Similarly, the peaks of equivalent blasting load of blastholes in the same section can be determined. The calculated equivalent blasting load is applied on the plane made up of the line of centers of blastholes in the same row and the blasthole axis (Lu *et al.* 2011, 2012). Then the peak P_b of equivalent blasting load of multi-blasthole explosion can be worked out through the formula below

$$P_b = (2r_0 / a) P_0 \quad (9)$$

where a is the pitch of blastholes, P_0 is the peak pressure of a single blasthole, and P_b is the peak pressure of equivalent load.

Single blasthole load model, which simulates blasting vibration by applying blasting load on a single blasthole wall, is hard to calculate due to the large amount and small size of blastholes in multi-blasthole explosion in tunnel engineering even when the nonlinear characteristics of rocks around the blasthole are ignored. Multi-blasthole load model, through applying the equivalent loads of blastholes in the same row on an equivalent plane, overcomes the nonlinear transformation of rocks around blasthole in single blasthole load model. As a result, it can avoid the burdensome mesh generation in numerical simulation and significantly reduces the workload in modeling and thus is widely used in the simulation of blasting vibration.

2.2 Determination method of multi-blasthole load model considering millisecond delay effect

To reduce the influences of blasting vibration on the surroundings, millisecond blasting is often used in the blasting of tunnel construction with adjacent existing buildings. The multi-blasthole load model commonly used currently only focuses on the analysis and simulation of blasting of blastholes (most of which are cut holes) in the same section. It fails to show the explosion processes in different sections and ignores the vibration attenuation effect caused by millisecond delay. Thus, in order to evaluate and predict the impact of tunnel explosion accurately, this paper, based on the equivalent blasting load proposed by Lu *et al.* (2011, 2012), puts forward a simplified multi-blasthole load model which has considered the millisecond delay effect in tunnel engineering.

In tunnel explosion, the explosive in a single blasthole will crush the rocks around it in the area 5 times the diameter of it and generate a blast wave near the explosion region. Therefore, the whole broken zone can be regarded as the explosion source. The blasting load can be simplified into a linear one and boosted to peak load. Then the time-history curve of blasting load can be calculated through the linearly unloaded triangle load (simplified into triangle load). The attenuated load is applied on the boundary of explosion source (a circle whose diameter is 5 times that of the blasthole).

As the cut holes in Section 1 differ from the blastholes

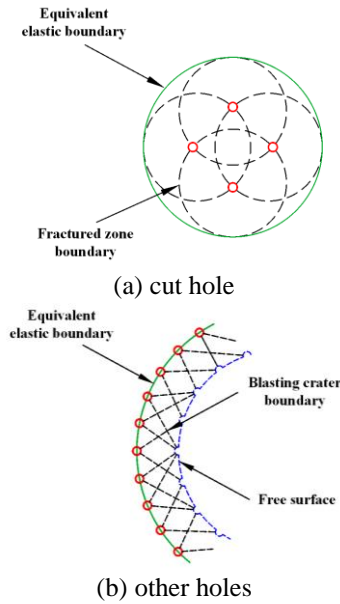


Fig. 4 Scheme of equivalent elastic boundary

in other sections, the blasting of cut holes will make a free face for the breaking holes explode soon afterwards. All the breaking holes, cushion holes and periphery holes detonate after the free face is created by the cut hole in Section 1. With the cracks in the free face and rocks caused by the blasthole explosion in the upper section, the explosion in the lower section cuts through the central axis of adjacent blastholes and thus the rocks cave. The time-history curves of equivalent loads of cut hole and non-cut hole on the equivalent boundary should be calculated differently.

(1) Determination of equivalent load curve of cut hole

Irrespective of the interaction between the blasting stresses of cut holes, a single cut hole can be seen an explosive cylinder which blasts in semi-infinite medium. Considering the synergistic effect of stress waves of different cut holes, the stress waves of cut holes are superimposed in certain proportion and evenly distributed on the equivalent elastic boundary (see Fig. 4(a)). According to the equivalence principle of force, the superposition proportion K can be expressed as

$$K = n \frac{2\pi r}{l} \quad (10)$$

where n refers to the amount of detonated blastholes in the cut hole section, r refers to the radius of broken zone and l refers to the perimeter of equivalent elastic boundary of the cut hole section.

The simplified triangle load curve is regarded as the time-history function of cut hole blasting load. The pressure rising time and unloading time of blasting load can be worked out through Eqs. (5) and (6) respectively. Then the time-history load on cut hole is equivalent to the time-history blasting load on the elastic boundary $P_e(t)$.

$$P_e(t) = n \frac{2\pi r}{l} P_b(t) \quad (11)$$

(2) Determination of equivalent load curve of non-cut

hole

As the cut hole explosion has made a free face for the non-cut holes which explodes afterwards, in which case, half of the loads on the circle of broken zone will transfer to the excavation contour face after the non-cut holes blast (see Fig. 4(b)). According to the equivalence principle of force and taking the simplified triangle load curve as the time-history function of blasting load of non-cut hole in one section, the pressure rising time and unloading time of blasting load can be obtained through Eqs. (5) and (6) respectively. Then the equivalent time-history load on the axial line of blasthole centers is given by

$$P_e(t) = n \frac{2r}{l} P_b(t) \quad (12)$$

where n is number of detonated blastholes in the non-cut hole section, r is the radius of broken zone, and l refers to the overall length of axial lines of blasthole centers.

(3) Determination of time-history curve of millisecond blasting load on excavation contour surface

The peak loads of cut hole and non-cut hole on equivalent elastic boundary can be obtained through Eqs. (11) and (12) respectively. Based on the attenuation law of stress wave, the attenuated peak loads of cut hole and non-cut hole can be worked out through Eqs. (7) and (8) respectively and then be applied on the tunnel excavation contour surface.

Suppose that the time blasting load transfers from blasthole wall to excavation contour surface is t_1 and the time difference of different sections caused by millisecond blasting is Δt , then delay time t the tunnel millisecond blasting load needs to reach the excavation contour surface is

$$t = t_1 + \Delta t \quad (13)$$

Based on the time obtained through Eq.(13), the blasting loads on the excavation contour surface of tunnel caused by the millisecond blasting of cut hole and non-cut hole in different sections are combined, through which a new tunnel blasting multi-blasthole load model considering millisecond delay effect is established.

3. Project case verification

3.1 Project Profile

The measured date of the upper center bench of Sailing Tunnel are used to verify the rationality of the multi-blasthole load model considering millisecond delay effect proposed in this paper. The Sailing Tunnel, located in Sanmenxia-Xichuan Highway, Henan Province, China, is a separated tunnel with small spacing. The distance between the left tube and right tube at exit and entrance are 18.33 m and 10.38 m, respectively. The elevation of Sailing Tunnel is 870~1120 m. The rocks around the tunnels are mainly Lower Proterozoic Quartz schist and have a monoclin structure. The joints at the entrance and exit of the tunnels are well developed.

The upper bench and lower bench of one Grade IV surrounding rock section in Sailing Tunnel are constructed

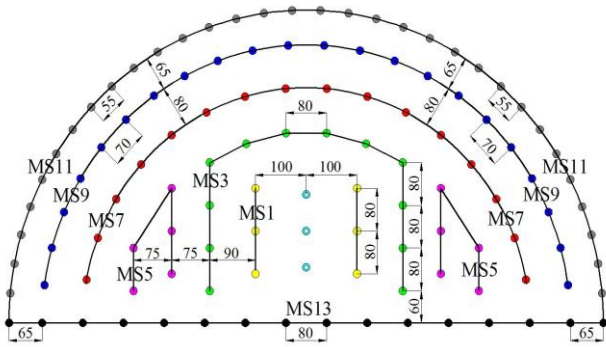


Fig. 5 The distribution of blastholes of Sailing Tunnel (unit: cm)

Table 1 Blasting parameters of the upper bench of sailing tunnel

Section	Blasthole			Charge amount	
	Category	Diameter	Amount	Single hole	Gross weight
		(mm)			
-	Empty hole	42	2	-	-
1	Cut hole	42	6	900	5.40
3	Cut hole	42	12	850	9.00
5	Satellite hole	42	10	600	6.00
7	Satellite hole	42	16	600	9.60
9	Inner ring hole	42	22	525	11.55
11	Periphery hole	42	32	375	12.00
13	Bottom hole	42	14	600	8.4
13	Bottom hole	42	2	600	1.20

Table 2 Explosive parameters

Explosive name	Density	Detonation wave velocity	Cartridge diameter
	(kg/m ³)	(m/s)	(mm)
2# Rock emulsion explosive	1000	3600	35

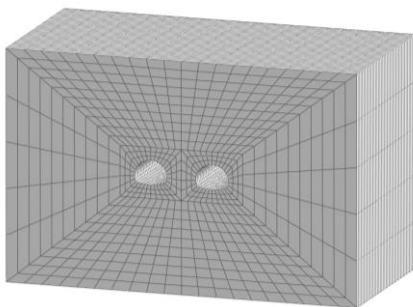


Fig. 6 Calculation meshes of finite element

Table 3 Rock mass parameters

Weight density	Elastic modulus	Poisson's ratio	Cohesion force	Friction angle
(KN/m ³)	(GPa)		(MPa)	(°)
23	1.5	0.35	0.5	30

and exploded separately using 2# rock emulsion explosive.

The distribution of blastholes is shown in Fig.5. The blasting vibration of the upper bench of Sailing Tunnel is analyzed through numerical simulation. The blasting parameters of the upper bench are listed in Table 1. The explosive parameters are given in Table 2.

3.2 Calculation model

The explosion process of Sailing Tunnel is simulated through the finite element software Midas/GTS NX. The constitutive model of rock mass is simulated through Mohr-Coulomb elastic-plastic model. The surrounding rock in the entrance section of the tunnels is thick bedded, and the joints are well developed. To simplify the calculation in the numerical simulation, the surrounding rock is analyzed as a homogeneous and isotropic material (Wu *et al.* 2015). According to the geological survey report, the recommended elastic modulus of the surrounding rock is 1.5-3.0 GPa. In numerical simulation, the elastic modulus of the rock is set to 1.5 GPa to consider the influence of joints on rock mechanical properties. To simulate the blasting vibration response at entrance of the tunnels, the corresponding geologic model is constructed (Fig. 6). The dimension of geologic model is 120 m×60 m×82 m (length×width×height). The tunnel section is an inverted arch with a single circle center. The tunnel diameter is 12 m. The actual distance between the two tunnels at entrance is 10.38 m. Taking into account the over excavation, the distance between the two tunnels in the constructed geologic model is set to 10 m. The burial depth of tunnel is 40 m. The distance between the tunnel and the boundaries on both sides are 42 m. Viscous damping boundary is used to determine the boundary conditions so as to simulate the general configuration of land, through which the accuracy of results will not be reduced by the stress wave reflection on boundary caused by blasting vibration. The rock mass parameters are listed in Table 3.

The time-history curve of load on the excavation contour line of Sailing Tunnel is worked out through the determination method of multi-blasthole load model which has considered millisecond delay proposed in this paper. The calculation steps are as follows: (1) work out the peak value of blasting load on blasthole wall through Eq. (2); (2) work out the attenuated blasting load on the boundary of broken zone through Eqs. (7) and (8); (3) taking the broken zone as explosion source and according to the attenuated blasting load on the boundary of broken zone, calculate the loads of blastholes in Section 1 and Sections 3-13 on the equivalent elastic boundary through Eqs. (11) and (12) respectively and then work out the peak value of the attenuated blasting load on excavation contour surface; (4) work out the pressure rising time and unloading time of blasting load through Eqs. (5) and (6) respectively; (5) according to the delay time of millisecond blasting and the propagation time of blasting load, calculate the time blasting load needs to reach excavation contour surface through Eq. (13).

The data of the equivalent blasting load on excavation contour surface of different sections are listed in Table 4. The time-history curve of blasting load is shown in Fig. 7. The delay time of Series I of China domestic millisecond electric detonator is used as the millisecond delay time of

Table 4 Data of blasting load

Type of load	Section	Peak load	Pressure rising time	Unloading time
		(MPa)	(ms)	(ms)
Millisecond blasting load	1	11.874	1.224	6.796
	3	14.190	1.220	6.708
	5	11.098	1.199	6.196
	7	7.057	1.199	6.196
	9	10.332	1.191	6.009
	11	17.577	1.171	5.560
13	12.690	1.199	6.196	
Triangle curve blasting load	-	11.754	1.513	17.252

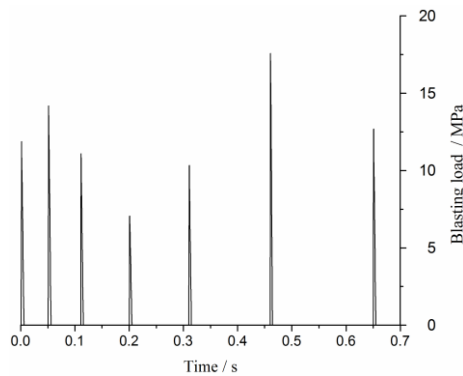


Fig. 7 Time-history curve of blasting load

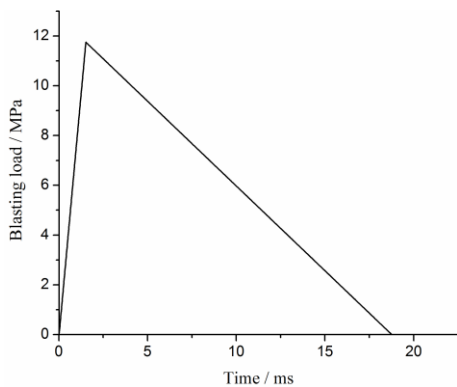


Fig. 8 Time-history curve of triangle blasting load

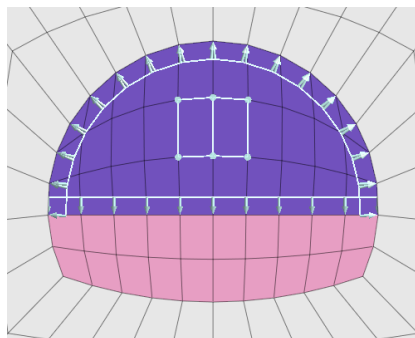


Fig. 9 The applying position of blasting load

electric detonator. For comparison, the data of blasting load obtained through triangle load function are given in Table 4 as well. The time-history curve of triangle blasting load is

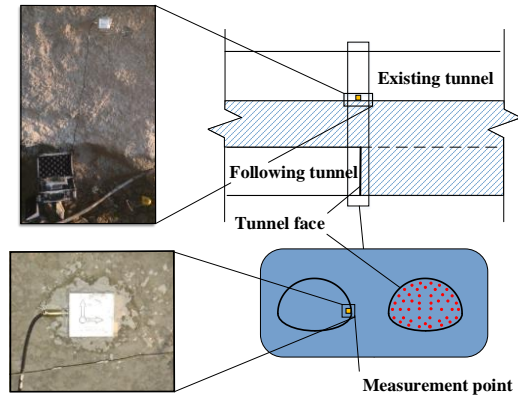


Fig. 10 The position of measurement point P and the arrangement

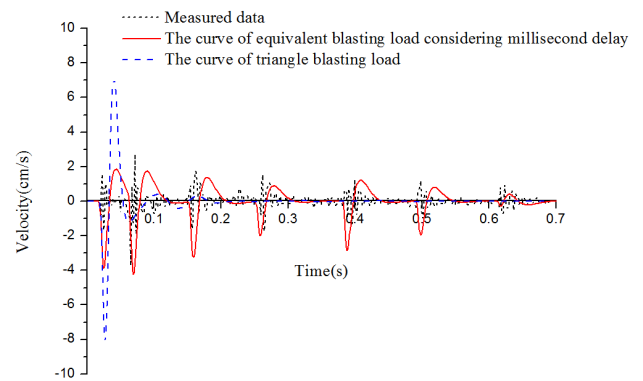


Fig. 11 Comparison of vibration velocity in the horizontal direction

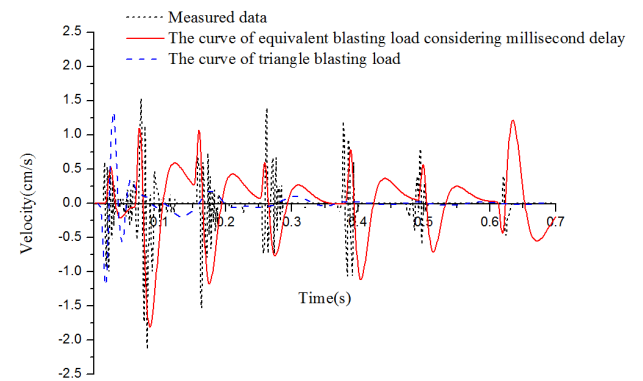


Fig. 12 Comparison of vibration velocity in the vertical direction

shown in Fig. 8. The applying position of equivalent blasting load on excavation surface is shown in Fig. 9.

3.3 Monitoring scheme of field blasting

The field blasting vibration detection instrument of Sailing Tunnel adopted in this paper is the TC-4850 Blasting Vibration Meter produced by Chengdu Zhongke Measurement and Control Co., Ltd. By fixing the sensor on the tested object with rigid connection, the sensor and the tested object will vibrate simultaneously, through which the sensor can collect the signal of blasting vibration and then transform it into electrical one and send it to the host. The

position of the typical measurement point P and the arrangement of the measurement point P in practical construction project are shown in Fig. 10.

3.4 Calculation results and analysis

The calculated results of vibration velocity of measurement point P in horizontal and vertical directions are compared with the measured ones. The comparisons of the vibration velocities of equivalent blasting load and triangle curve blasting load as well as the measured blasting vibration velocity in horizontal and vertical direction are respectively shown in Figs. 11 and 12.

As shown in Fig. 11, the horizontal vibration caused by the equivalent blasting load which has considered millisecond delay effect and the measured one basically accord with each other in change rule. The two curves accord with each other as well in the occurrence time and amount of wave crests and troughs. Besides, the peaks of vibration velocity are both caused by the cut hole explosion in the second section. In conclusion, the calculation results agree well with the measured ones and the error is small. However, the triangle curve blasting load is much larger in horizontal vibration velocity than the measured blasting load as it fails to consider the millisecond delay time effect. The error is large.

As shown in Fig. 12, the vertical vibration caused by the equivalent blasting load which has considered millisecond delay effect and the measured data accord with each other in change rule. Besides, the two curves also accord well in the peak of vibration velocity. However, the vibration caused by triangle curve blasting load differs a lot from the measured one in both change rule and numerical value.

It can be known from the time-history curve of vibration that the peak velocity of vibration (4.25 cm/s in horizontal direction; 1.81 cm/s in vertical direction) caused by the explosion in Section 3 is large than that (1.95 cm/s in horizontal direction; 0.72 cm/s in vertical direction) caused by the explosion in Section 11. That's because the pressure rising time and unloading time of the explosion of the second section are both longer than those of Section 11 (see Fig. 4). As a result, the impulse of blasting load of the second section is larger than that of Section 11. In addition, the difference between the field data and the numerical results may also be related to the simplification of the surrounding rock defined as a homogeneous and isotropic material in numerical simulation.

The comparison of the vibration velocities of equivalent blasting load considering millisecond delay effect, triangle curve blasting load, and measured blasting load in horizontal direction and vertical direction is shown in Table 5.

As shown in Table 5, the peak velocity of horizontal vibration caused by the equivalent blasting load considering millisecond delay effect is 4.25 cm/s and is 15.5% higher than the measured result (3.68 cm/s). The velocity of horizontal vibration caused by triangle curve blasting load is 8.03 cm/s and is 118.2% higher than the measured result. The peak velocity of vertical vibration caused by the equivalent blasting load considering millisecond delay effect and that caused by triangle curve blasting load

Table 5 Comparison of vibration velocity data

Direction	Peak velocity of vibration			Error	
	(cm/s)			Millisecond blasting equivalent load	Triangle curve load
	Millisecond blasting equivalent load	Triangle curve load	Measured blasting load		
Horizontal	4.25	8.03	3.68	15.5%	118.2%
Vertical	1.81	1.33	2.16	16.2%	38.4%

respectively are 1.81 cm/s and 1.33 cm/s. They are 16.2% and 38.4% lower than the measured result (2.16 cm/s) respectively.

According to the above analysis, the vibration caused by the equivalent blasting load considering millisecond delay effect accords with the measured one in change rule. Besides, the calculated peak velocity of vibration is close to the measured result. The error is small. Therefore, conclusions can be drawn that the proposed determination method of equivalent blasting load which has considered millisecond delay effect is reasonable and feasible.

4. Effects of millisecond delay on vibration velocity

It can be known from Figs. 11 and 12 that through controlling the orders and intervals of millisecond blasting in different sections, the superimposition of blasting vibration can be effectively avoided and thus reduce the peak velocity of blasting vibration. Therefore, conclusions can be drawn that millisecond blasting can effectively control the blasting vibration and reduce its effect on adjacent buildings. The influence rule of millisecond delay on blasting vibration needs further study. Based on the construction blasting of the upper bench of Sailing Tunnel on Sanmenxia-Xichuan Expressway, the following sections attempt to analysis the influence rule of different millisecond blasting delay time on blasting vibration through numerical simulation. The millisecond delay time used in the numerical calculation respectively is 10 ms, 30 ms and 50 ms. Fig.13 shows the horizontal vibration curve of Measurement Point P with millisecond delay of 10 ms, 30 ms, and 50 ms. For comparison, the horizontal vibration curve of P with the millisecond delay time of Series I of China domestic millisecond electric detonator is shown in Fig.13 as well.

It can be known from Fig. 13 that there are no significant differences among the peak velocities of vibration in horizontal direction caused by blasthole explosion in the Section 1 under different millisecond delay time. These peak velocities accord with that under the millisecond delay of Series I domestic millisecond electric detonator. However, the velocities caused by the explosion in the later sections are quite different due to different millisecond delay time. When the millisecond delay time is 50 ms, the peak velocity of blasting vibration is 4.41 cm/s, which is slightly different from the peak velocity of vibration (4.25 cm/s) using the millisecond delay time of Series I of China domestic millisecond electric detonator. The peak velocities of vibration in later sections only differ in the occurrence time instead of value. It indicates that the

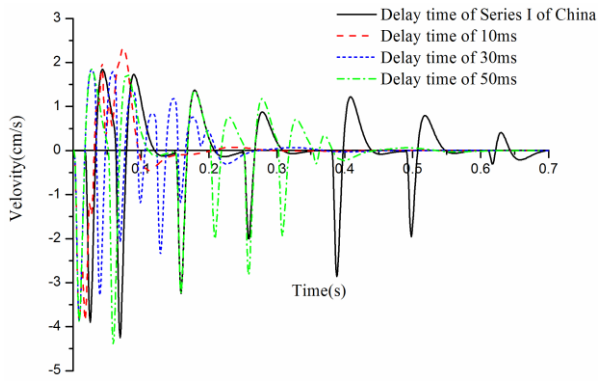


Fig. 13 Horizontal vibration curve of measurement point P with different millisecond delay time

Table 6 The occurrence time of the wave crests and troughs of horizontal vibration velocity

Section	Waveform	Velocity (cm/s)	Occurrence time (s)	Interval (ms)	Delay time of Series I of China domestic millisecond electric detonator (ms)	Corrected millisecond delay time (ms)
1	Wave trough	-3.89	0.025	-	0	0
	Wave crest	1.84	0.043	26		
3	Wave trough	-4.25	0.069	-	50	20
	Wave crest	1.73	0.089	70		
5	Wave trough	-3.24	0.159	-	110	40
	Wave crest	1.37	0.179	80		
7	Wave trough	-2.00	0.259	-	200	60
	Wave crest	0.88	0.279	109		
9	Wave trough	-2.86	0.388	-	310	80
	Wave crest	1.22	0.408	90		
11	Wave trough	-1.95	0.498	-	460	100
	Wave crest	0.80	0.518	99		
13	Wave trough	-0.30	0.617	-	650	120
	Wave crest	0.41	0.63	-		

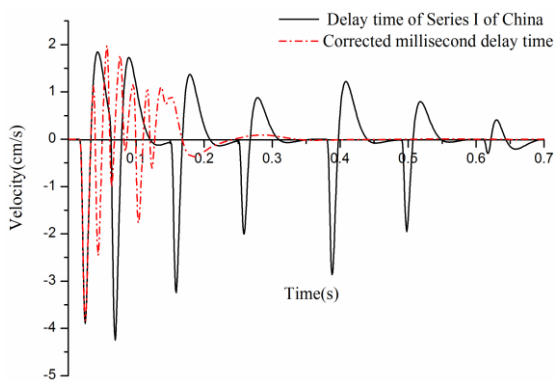


Fig. 14 Horizontal vibration curve of measurement point P with corrected millisecond delay time

millisecond delay time 50 ms is able to separate the explosions in different sections and reduce the mutual effect effectively. When the millisecond delay time is 30 ms or 10 ms, the explosion in different sections will influence each

Table 7 Horizontal vibration velocity of point P with different millisecond delay times

Section	Wave form	Delay time of Series I of China domestic millisecond electric detonator	Millisecond delay time of 10 ms	Millisecond delay time of 30 ms	Millisecond delay time of 50 ms	Corrected millisecond delay time
		(cm/s)	(cm/s)	(cm/s)	(cm/s)	(cm/s)
1	Wave trough	-3.89	-3.89	-3.89	-3.89	-3.89
	Wave crest	1.84	-	1.85	1.84	1.13
3	Wave trough	-4.25	-3.85	-3.28	-4.41	-2.45
	Wave crest	1.73	-	1.79	1.76	1.98
5	Wave trough	-3.24	-1.45	-2.07	-3.23	-0.91
	Wave crest	1.37	0.99	1.39	1.36	1.77
7	Wave trough	-2.00	-	-1.18	-2.01	-0.26
	Wave crest	0.88	1.99	0.85	0.77	1.17
9	Wave trough	-2.86	-	-2.34	-2.82	-1.76
	Wave crest	1.22	1.20	1.19	1.18	1.09
11	Wave trough	-1.95	-	-1.17	-1.93	-0.63
	Wave crest	0.80	2.33	0.77	0.71	1.11
13	Wave trough	-0.30	-0.451	-	-0.30	-0.384
	Wave crest	0.41	-	0.46	0.35	0.09

other greatly. The shorter the millisecond delay time, the greater the mutual influence.

In conclusion, the delay time of millisecond blasting of each section will, to a certain extent, influence the blasting vibration. Through a proper control of millisecond delay time, the wave trough of the blasting vibration curve of the later section and the wave crest of the blasting vibration curve of the former section will appear at the same time, then the wave trough and wave crest will be superimposed and counteracted, thus reducing the effect of blasting vibration. Based on the upper bench blasting of Sailing Tunnel on Sanmenxia-Xichuan Expressway mentioned in Section III, this paper, through the delay time of Series I of China domestic millisecond electric detonator, works out the millisecond blasting delay time of different sections suitable for the project. The calculation steps are as follows: (1) extract the occurrence time of wave crest and trough of vibration curve caused by the explosion of Series I domestic millisecond electric detonator in different sections; (2) work out the time interval Δt_i between the occurrence time of the wave trough (the later section) and the wave crest (the former section) of two adjacent sections; (3) according to the millisecond delay time of blasting ΔT_i , work out the initiation millisecond delay time ΔL_i which can superimpose the wave trough of vibration curve of the later section and the wave crest of vibration curve of the former section through Eq. (14).

$$\Delta L_i = \Delta T_i - \Delta t_i \tag{14}$$

The occurrence time of wave crest and trough of horizontal vibration velocity of measurement point P is given in Table 6. Calculated through Eq. (14), the millisecond delay time which enables the wave trough (the

later section) and the wave crest (the former section) of two adjacent sections appear at the same time, i.e., the corrected millisecond delay time, is also give in Table 6. It can be known from Table 6 that the corrected millisecond delay time of different sections is 20 ms. That's because the oscillation periods of the blasting vibration of different sections in this study are 40-50 ms. The interval between the occurrence time of wave crest and wave trough of the same section is about 20 ms.

The comparison of the horizontal vibration curves of point P which is obtained through the corrected millisecond delay time listed in Table 6 and the delay time of Series I of China domestic millisecond electric detonator is shown in Fig.14. It can be known from Fig.14 that the wave troughs of the two vibration curves overlap in Section 1. However, in the other sections, the two vibration curves are staggered and do not influence each other. The peak velocity caused by the blasting vibration of Section 3 is the highest (4.25cm/s). In the blasting vibration curve with corrected millisecond delay time, the vibrations of adjacent sections interplay. The wave trough of the later section and the wave crest of the former section overlap and thus reduce the peak velocity (the peak velocities of other sections except Section 1 are below 2.5 cm/s). Therefore, the vibration is reduced.

Table 7 gives the statistical data of the horizontal peak velocity of point P under different millisecond delay times (the millisecond delay time of Series I of China, the millisecond delay time of 10, 30, 50 ms and the corrected millisecond delay time). It can be seen from Table 7 that the wave trough velocities in section 1 are the same under different millisecond delay times. For the millisecond delay time of 10 ms, because the vibration curves overlap each other, the wave crest in sections 1, 3 and 13 and wave trough in sections 7, 9 and 11 do not appear. The peak velocities (wave crest and wave trough) calculated from the millisecond delay time of 30 and 50 ms are very close to that calculated from the millisecond delay time of Series I of China in different sections. From the overall perspective, the peak velocities calculated from the corrected millisecond delay time are relatively small in the later sections (except for section 1) and the maximum velocity is 2.45 cm/s, while the maximum velocity under the millisecond delay time of Series I of China, the millisecond delay time of 10, 30, 50ms in the later sections are respectively 4.25, 3.85, 3.28 and 4.41 cm/s. Therefore, the blasting vibration can be effectively controlled by setting reasonable millisecond delay time.

In conclusion, the wave trough of the later section and the wave crest of the former section will appear at the same time if the millisecond blasting delay time is controlled properly. In that case, the wave trough and crest are superimposed and counteracted, thus reducing the blasting vibration. It provides a new solution for reducing the effects of blasting on the vibration of adjacent existing buildings. In short-distance blasting construction, the blasting vibration parameters of each section can be obtained through trial explosion. A back analysis is carried out through numerical simulation. Then, the delay time of millisecond blasting can be determined through the distance between the blasting position and adjacent existing buildings together with explosive parameters.

5. Conclusions

- Based on Saint-Venant's Principle and equivalence principle of force, this paper proposes a determination method of equivalent load of blasting vibration considering millisecond delay effect.

- The proposed method, based on the equivalence principle of elastic-static force of stress wave, equals the loads of single blastholes of the same section to the triangle blasting load curve applied on the exploded equivalent elastic boundary surface. Based on the attenuation law of stress wave, it applies the attenuated equivalent elastic blasting load curve on the tunnel contour surface. Then by taking the millisecond delay time of different sections into account, the time-history curve of equivalent load of the whole section considering the millisecond delay effect is obtained.

- The blasting vibration of Sailing Tunnel on Sanmenxia-Xichuan Expressway is calculated through numerical simulation. The calculation results are compared with the measured ones. It is known from the comparison that the vibration caused by equivalent blasting load which has considered millisecond delay effect agrees well with the measured one in change rule. Besides, the calculated peak velocity of vibration is close to the measured one and the error is small. The analysis of this engineering project proves that the proposed determination method of equivalent blasting load which has considered millisecond delay effect is reasonable and feasible.

- The analysis of millisecond blasting at different time intervals indicates that, through setting a proper millisecond blasting delay time, the wave trough of vibration curve of the later section and the wave crest of vibration curve of the former section will appear at the same time. Then the wave trough and crest can overlay and be counteracted, thus reducing the blasting vibration.

It should be pointed out that during the initiation process of tunnel millisecond blasting, the surrounding rocks will be damaged by the explosion in the former section before the initiation of explosion in the later section. In that case, the rock damage and degradation, together with the deterioration of rock formation will affect the determination of the blasting load. Thus, further studies are needed as this paper fails to consider the rock damage in calculation. Moreover, in the subsequent research, the influence of joints and anisotropic characteristics of the rock on blasting vibration response will be discussed.

Acknowledgements

The present work is subsidized and supported by the National Natural Science Foundation of China (Nos. 51578447, 51404184, 51308443), the Youth Science and Technology Nova Program of Shaanxi Province (No. 2018KJXX-40), the Natural Science Basic Research Program of Shaanxi Province (No. 2016JQ4009) and the Specialized Scientific Research Program of Education Department of Shaanxi Provincial Government (No. 14JK1401). The financial supports are gratefully acknowledged by the authors!

References

- Ak, H., Iphar, M., Yavuz, M. and Konuk, A. (2009), "Evaluation of ground vibration effect of blasting operations in a magnesite mine", *Soil Dyn. Earthq. Eng.*, **29**(4), 669-676.
- Banadaki, M.D. and Mohanty, B. (2012), "Numerical simulation of stress wave induced fractures in rock", *J. Impact Eng.*, **40**, 16-25.
- Cardu, M. and Seccatore, J. (2016), "Quantifying the difficulty of tunnelling by drilling and blasting", *Tunn. Undergr. Sp. Technol.*, **60**, 178-182.
- Henrych, J. (1979), *The Dynamics of Explosion and its Use*, Elsevier Scientific Publishing Company, New York, U.S.A.
- Jiang, N. and Zhou, C. (2012), "Blasting vibration safety criterion for a tunnel liner structure", *Tunn. Undergr. Sp. Technol.*, **32**, 52-57.
- Kuzu, C. and Guclu, E. (2009), "The problem of human response to blast induced vibrations in tunnel construction and mitigation of vibration effects using cautious blasting in half-face blasting rounds", *Tunn. Undergr. Sp. Technol.*, **24**(1), 53-61.
- Li, X.L., Wang, E.Y., Li, Z.H., Bie, X.F., Chen, L., Feng, J.J. and Li, N. (2016), "Blasting wave pattern recognition based on Hilbert-Huang transform", *Geomech. Eng.*, **11**(5), 607-624.
- Li, X.P., Chen, J.H., Li, Y.H. and Dai, Y.F. (2010), "Study of blasting seismic effects of underground chamber group in Xiluodu hydropower station", *Chin. J. Rock Mech. Eng.*, **29**(3), 494-500 (in Chinese).
- Ling, T.H. and Li, X.B. (2004), "Time-energy analysis based on wavelet transform for identifying real delay time in millisecond blasting", *Chin. J. Rock Mech. Eng.*, **23**(13), 2266-2270 (in Chinese).
- Lu, W.B., Yang, J.H., Chen, M. and Zhou, C.B. (2011), "An equivalent method for blasting vibration simulation", *Simul. Model. Pract. Th.*, **19**(9), 2050-2062.
- Lu, W.B., Yang, J. H., Yan, P., Chen, M., Zhou, C.B., Luo, Y. and Jin, L. (2012), "Dynamic response of rock mass induced by the transient release of in-situ stress", *J. Rock Mech. Min. Sci.*, **53**, 129-141.
- Ma, G.W. and An, X.M. (2008), "Numerical simulation of blasting-induced rock fractures", *J. Rock Mech. Min. Sci.*, **45**(6), 966-975.
- Nateghi, R., Kiany, M. and Gholipouri, O. (2009), "Control negative effects of blasting waves on concrete of the structures by analyzing of parameters of ground vibration", *Tunn. Undergr. Sp. Technol.*, **24**(6), 608-616.
- Ozer, U. (2008), "Environmental impacts of ground vibration induced by blasting at different rock units on the Kadikoy-Kartal metro tunnel", *Eng. Geol.*, **100**(1), 82-90.
- Ramulu, M., Chakraborty, A.K. and Sitharam, T.G. (2009), "Damage assessment of basaltic rock mass due to repeated blasting in a railway tunnelling project-A case study", *Tunn. Undergr. Sp. Technol.*, **24**(2), 208-221.
- Resende, R., Lamas, L.N., Lemos, J.V. and Calçada, R. (2010), "Micromechanical modelling of stress waves in rock and rock fractures", *Rock Mech. Rock Eng.*, **43**(6), 741-761.
- Resende, R., Lamas, L., Lemos, J. and Calçada, R. (2014), "Stress wave propagation test and numerical modelling of an underground complex", *J. Rock Mech. Min. Sci.*, **72**, 26-36.
- Rodríguez, R., Toraño, J. and Menéndez, M. (2007), "Prediction of the airblast wave effects near a tunnel advanced by drilling and blasting", *Tunn. Undergr. Sp. Technol.*, **22**(3), 241-251.
- Saharan, M.R. and Mitri, H.S. (2008), "Numerical procedure for dynamic simulation of discrete fractures due to blasting", *Rock Mech. Rock Eng.*, **41**(5), 641-670.
- Sainoki, A. and Mitri, H.S. (2014), "Numerical simulation of rock mass vibrations induced by nearby production blast", *Can. Geotech. J.*, **51**(11), 1253-1262.
- Sanchidrian, J.A., Segarra, P. and López, L.M. (2007), "Energy components in rock blasting", *J. Rock Mech. Min. Sci.*, **44**(1), 130-147.
- Song, Z.P., Yang, T.T. and Jiang, A.N. (2016), "Elastic-plastic numerical analysis of tunnel stability based on the closest point projection method considering the effect of water pressure", *Math. Prob. Eng.*, 1-12.
- Wang W.L. (1984), *Drill and Blasting*, Coal Industry Press, Beijing, China (in Chinese).
- Wu, Z., Liang, X. and Liu, Q. (2015), "Numerical investigation of rock heterogeneity effect on rock dynamic strength and failure process using cohesive fracture model", *Eng. Geol.*, **197**, 198-210.
- Yang, J., Lu, W., Chen, M., Yan, P. and Zhou, C. (2013), "Microseism induced by transient release of in situ stress during deep rock mass excavation by blasting", *Rock Mech. Rock Eng.*, **46**(4), 859-875.
- Yilmaz, O. and Unlu, T. (2013), "Three dimensional numerical rock damage analysis under blasting load", *Tunn. Undergr. Sp. Technol.*, **38**, 266-278.

CC